DECAPITATED IMPACTORS IN THE LABORATORY AND ON THE PLANETS; P.H. Schultz, Brown University, Providence, RI 02912 and D.E. Gault, Murphys Center of Planetology, Murphys, CA 95247.

Background: The partitioning of energy during oblique impacts is very different from vertical impacts. For vertical impacts into sand, about 73% of the initial impactor energy is expended in target displacement including 20% in compaction and 53% in ejecta (1). The remaining energy (27%) is partitioned into waste heat and kinetic energy of the projectile. At low impact angles (15° from the horizontal), however, most of the impactor energy occurs as kinetic energy in ricocheted debris (2, 3). Internal energy in the projectile decreases as $\sin^2\theta$ until ricocheting nearly intact at very low impact angles (<7.5°), even at hypervelocities (>6 km/s) into non-porous targets (3). Oblique impacts of ductile aluminum into solid aluminum targets have been observed to consistently produce nearby downrange pits (2, 4). Because these enigmatic pits occur within a few projectile diameters of first contact, they cannot be caused by hypervelocity ballistic ejecta from the target. They appeared to be produced instead by decapitation of the projectile due to spallation.

Laboratory Experiments: Positioning the target edge close to the expected downrange rim of the primary crater permitted isolating the downrange impacting fragments from the first impact. Vertical witness plates placed farther downrange recorded the dispersion and trajectories of these isolated fragments. High-frame rate imaging from 35,000 fps to 2×10^6 fps (frames per second) constrained their velocity within about 5% and permitted deriving the size of the fragments from the size of the impact pits through scaling relations for identical materials (5). Aluminum and pyrex spheres (0.635 cm spheres) were launched at hypervelocities (~5 km/s) in order to contrast the response of ductile and brittle materials. Aluminum targets included a range of thicknesses (from 0.079 to 2.5 cm) in order to explore first-order effects of initial contact. Different targets (soft aluminum, sand, and water) were also used to calibrate compositional effects.

High velocity impact (5–6 km/s) of 0.635 cm aluminum spheres into 2.5 cm thick aluminum targets produce a characteristic ricochet pattern with a horizontal concentration and vertical strings of more isolated impact pits. Isolation of the downrange second impacts, however, produced only a faint horizontal line of very small pits. In such cases, the largest pits occurred well below the impact surface plane and only slightly (but significantly) above the projected intercept of the original impactor trajectory. For thin targets (less than 0.5 projectile diameter), the observed vertical offset depended more on proximity to the target edge than on target composition or thickness. The vertical offset resulting from impacts into thick aluminum targets typically correspond to a 10° change from the original trajectory. High frame-rate photography revealed that the velocity of the fragments were indistinguishable from the launch velocity, i.e., a loss of no more than 300 m/s. This record also clearly distinguished the high-speed (9 km/s) jetting component from a lower speed (~3 km/s) cloud of expanding self-luminous ejecta directed along the impact plane. The latter component was observed to uniformally plate the witness plate and pits with a microscopically thin layer of aluminum.

Discussion: The laboratory experiments clearly demonstrated that the downrange ricochet pits indeed result from spallation of the top of the projectile. At a 15° impact angle, decapitation produces a bimodal distribution with 4 to 8 fragments of nearly equal size and numerous smaller debris. Because these fragments did not impact the target surface, larger fragments survive (Figure 1). The small near-vertical velocity component of the spalled debris is generally consistent with calculated peak pressures based on the approach of Gault and Heitowit (6) modified to include only the vertical velocity component. For 5 km/s impact velocities, the shock created by first contact reaches the top of the projectile before it has penetrated 10% of its diameter into the surface. Even brittle and fragile pyrex spheres exhibited surviving fragments 10–20% of the original projectile diameter at 5.4 km/s and 15°. We note that oblique impacts into easily volatized targets (plasticene, water, carbonates) in addition produce a significant boost to the spall velocity, most likely due to acceleration in the observed impact-generated vapor cloud (7).

Hence, internal energy losses in the projectile appear to decrease for oblique impacts owing to spallation of the free surface. Several observations suggest, however, that internal energy losses along the projectile/target interface increase. First, the photographic records reveal a self-luminous ejecta cloud separable from the jetting phase that expands non-ballistically—even below the target reference surface. Second, aluminizing of thin pyrex witness plates placed just 2.5 cm above the impact indicate considerable internal but little kinetic energy in the expanding ejecta cloud. And third, downrange discoloration of the target occurs within a broad parabolic-shaped fan. This discoloration suggests brief but intense heating related to ejecta, not target-transmitted shock heating. Hence, the decrease in projectile fragmentation with decreasing impact angle down to 15° is paradoxically accompanied by an increase in heating, even for impacts into aluminum where calculated peak shock pressures are sufficient to induce only partial melting (1). This heating is expressed not only by jetting but also by fine incandescent (perhaps even melted and vaporized) aluminum ejecta. We attribute such heating to mechanical shear, a process commonly used to weld dissimilar materials, and we suspect that internal losses by shear heating may exceed shock-induced losses for impact angles less than 20–30°.

The downrange patterns resulting from projectile spallation observed in the laboratory have

striking analogs in the planetary record. Re-examination of the oblique impact record on the Moon and Mars reveals numerous examples of downrange re-impacts. The specific pattern depends on local topography and crater size. On flat surfaces, nearby and downrange oblique impact are readily recognized (Fig. 2a). At low impact angles, however, local slopes can significantly affect not only the distance between first and ricochet impact but also can change the impact angle of decapitation fragments. Ricochet from oblique impacts on the floors of several large martian craters exhibit re-impact craters on the facing wall that are even larger than the crater resulting from the initial impact. In contrast, downslope collisions have produced a succession of smaller, shallower impacts (Fig. 2b). At the broadest scales, the initial impact and downrange re-impact merge. Orcus Patera (450 km x 150 km) on Mars exhibits the diagnostic ejecta pattern for an oblique impact and a series of smaller coalescing impacts downrange. The crater Schiller on the Moon is accompanied by a series of larger downrange, coalescing craters due to the topographic effects of the facing wall/ring of Schiller basin. Both morphologies can be understood in terms of the processes observed in the laboratory. Although it can be argued that such (or some) companion impacts reflect multiple impacts by tidally disrupted or binary asteroids, the consistent pattern of smaller/shallower impacts downrange on flat surfaces, the sequence of impact, and the observed controlling effects of topography all support a process analogous to projectile decapitation observed in the laboratory.

Concluding Remarks: Laboratory experiments reveal fundamental differences in the partitioning of energy with impact angle and can be supported by both first-order theoretical considerations and planetary analogs. We feel that the process and observed phenomena provide more than just an explanation for enigmatic or unique impact structures. The decreased disruption and ricochet of a single basin-forming impactor at low angles (<15°) could contribute significantly to a sibling population of impactors, particularly in satellite systems (see 8). The increased partitioning of energy into shear heating at more modest angles (10–30°) could affect the formation and recycling of planetary atmospheres (9). Finally, the combination of vapor release and embedded projectile ricochet provides a mechanism for episodically creating orbiting debris around solid-surface planets that could evolve into a short-lived ring (3, 10).

References: (1) Braslau, D. (1970) *J. Geophys. Res. 75*, 3987–3999. (2) Gault, D.E. and Wedekind, J. (1978) *Proc. Lunar Planet. Sci. Conf. 9th*, 3843–3875. (3) Schultz, P.H. and Gault, D.E. (1990) In *Proc. of Catastrophes in Earth History, Geol. Soc. Sp. Paper* (in press). (4) Summers, J.L. (1959) NASA TND-94. (5) Denardo, B.P. *et al.* (1967) *NASA TND-4067*. (6) Gault, D.E. and Heitowit, E.D. (1963) *Proc. Sixth Hypervelocity Impact Symp., Vol. 2*, 419–456. (7) Schultz, P.H. (1988) In *Lunar and Planet. Sci. XIX*, LPI, Houston, 1039–1040. (8) Halfen, C. *et al.* (1990) In *Lunar and Planet. Sci. XXI*, LPI, Houston (this volume). (9) Schultz, P.H. (1988) *Eos, 69*, p. 388. (10) Schultz, P.H. *et al.* (1990) In *Lunar and Planet. Sci. XXI*, LPI, Houston (this volume).

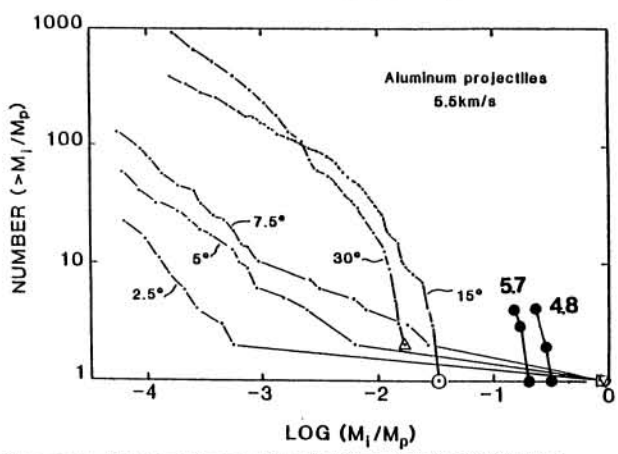

Figure 1. Size distribution of ricocheting projectile resulting from oblique impacts (referenced to horizontal) of sand (dots) and 2.5 cm-thick aluminum (large filled circles) targets. For impacts into aluminum targets, the ricochet component was prevented from re-impacting the target surface, thereby preserving the actual size and trajectory of the spalled projectile. Only the four largest spall fragments are shown for two different velocities.

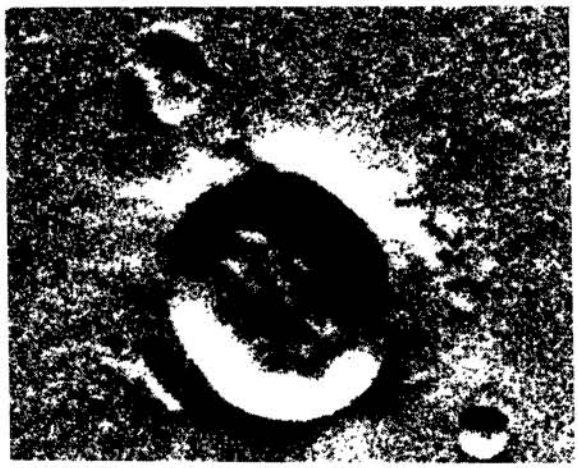

Figure 2a. Numerous craters on Mars exhibit evidence for downrange impact by spall fragments from the top of the projectile. Figure 2a shows a 4.2 x 5.5 km diameter crater with companion downrange impact (387B06).

Figure 2b. Illustrates a 15 x 35 km-diameter crater that impacted the downsloping wall of Kasai Vallis (519A27). Although appearing to be the consequence of multiple impacts, the same pattern can be reproduced in the laboratory by successive spallation and impact of a single projectile.